Radio channel measurements at street intersections for vehicle-to-vehicle applications

Kåredal, Johan; Tufvesson, Fredrik; Abbas, Taimoor; Klemp, Oliver; Paier, Alexander; Bernadó, Laura; Molisch, Andreas

Published in:
IEEE 71st Vehicular Technology Conference (VTC 2010-Spring), 2010

DOI:
10.1109/VETECS.2010.5493955

2010

Radio Channel Measurements at Street Intersections for Vehicle-to-Vehicle Safety Applications

Johan Karedal[1], Fredrik Tufvesson[1], Taimoor Abbas[1], Oliver Klemp[2], Alexander Paier[3], Laura Bernadó[4], and Andreas F. Molisch[5]

[1]Dept. of Electrical and Information Technology, Lund University, Lund, Sweden.
[2]Delphi Delco Electronics Europe GmbH, TecCenter, Bad Salzdetfurth, Germany.
[3]Institut für Nachrichtentechnik und Hochfrequenztechnik, Technische Universität Wien, Vienna, Austria.
[4]Forschungszentrum Telekommunikation Wien (FTW), Vienna, Austria.
[5]Dept. of Electrical Engineering, University of Southern California, Los Angeles, CA, USA.

***Abstract*—This paper presents the results of an empirical study of wireless propagation channels for vehicle-to-vehicle communications in street intersections, a scenario especially important for collision avoidance applications. The results are derived from a channel measurement campaign performed at 5.6 GHz in four different types of urban intersections.**

We present results on typical power delay profiles, pathloss and delay spreads and discuss important propagation mechanisms. By comparing the results of the different intersections, we find that absence of line-of-sight is problematic for system coverage, especially when there are few other significant scattering objects in and around the intersection. Roadside buildings can create important propagation paths that account for a considerable part of the total received power.

I. Introduction

Vehicle-to-vehicle (V2V) communications are envisioned for use in the context of Intelligent Transportation Systems (ITS) and have attracted a lot of interest in recent years. Many applications are envisioned for traffic safety enhancement, where the idea is that vehicles can facilitate their driving by sharing traffic information, e.g., coordinate and velocity vectors, via wireless links. Of particular interest are *collision avoidance* systems that detect if two vehicles are on a collision course, in which case warnings are issued to the respective drivers. Such systems are particularly useful in *street intersections*, especially where the optical line-of-sight (LOS) between approaching vehicles is absent.

The reliability of collision avoidance systems is, however, ultimately dictated by the properties of the wireless propagation channel. Hence, the channel conditions that can be expected needs to be evaluated before any conclusions can be drawn regarding the feasibility of such systems. Whereas recent years have seen a number of measurement campaigns for V2V systems, most existing measurement campaigns have focused on communication between cars driving either in convoy (e.g., [1], [2], [3], [4]) or in opposite, though parallel, directions (e.g., [5], [6]). A theoretical analysis of propagation channels in intersections was presented in [7], whereas [8] presented some results from V2V measurements between one car approaching an urban intersection and one parked around a corner. To the authors' best knowledge, no measured channel properties have been presented for the case where two cars are approaching an intersection on a collision course, as would be the most interesting case for a real collision avoidance application. The current paper alleviates this gap by presenting the results of extensive measurements performed in four different types of intersections in the cities of Lund and Malmö, Sweden. The measurement campaign was performed with cars and antennas chosen to constitute as realistic a setup as possible. Regular cars equipped with antennas especially designed for V2V communication, which were integrated into the regular roof-top antenna module, were used.

We analyze the wireless propagation channel between two cars approaching an intersection from perpendicular directions and present typical power delay profiles where we discuss the most important propagation paths. We also present measured pathloss and delay spreads for all intersections. Particular focus is put on the differences between the channel properties in the different intersection types.

The remainder of the paper is organized as follows: In Section II we describe the measurement setup in detail. Especially, we point out the physical differences between the four intersections. In Section III we describe the evaluation of the measurement data, i.e., how we derive the results presented in Section IV. Finally, the paper is wrapped up with a summary and conclusions in Section V.

II. Channel Measurements

A. Measurement Equipment

Channel samples were recorded using the RUSK Lund channel sounder that performs multiple-input multiple-output (MIMO) measurements based on the switched array principle. The channel sounder recorded the complex, time-varying channel transfer function $H(f,t)$ over a frequency band of 240 MHz centered around 5.6 GHz, the highest center frequency allowed by the sounder. This was assumed close enough to the 5.9 GHz band dedicated to V2V communications, in both Europe and the USA, for no significant differences to be expected. The test signal length was set to 3.2 μs, which

This work was partially funded by the Vienna Science and Technology Fund (WWTF) in the FTW project COCOMINT, partially by the SSF center for High-Speed Wireless Communication and was carried out in cooperation with the FTW project ROADSAFE and the Christian Doppler Laboratory for Wireless Technologies for Sustainable Mobility.

978-1-4244-2519-8/10/$26.00 ©2010 IEEE

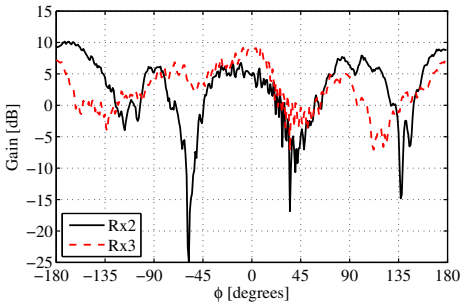

Fig. 1. Azimuth antenna patterns for the middle two elements of the Rx array (the Tx elements are similar) at 5.6 GHz; ϕ is the azimuth angle and $\phi = 0$ degrees is the forward direction of the car(s).

allows for a maximum resolvable delay of 960 m, and the output power was 27 dBm. The sounder sampled the channel at 769 frequency points during 10 or 20 seconds (in different measurements), using a time increment of $\Delta t = 0.3072$ ms.

The cars and antennas used in the measurements were chosen with the intention of constituting a realistic user scenario. Two regular cars in hatchback style (with a height of 1.73 m) were used, each equipped with a four-element linear antenna array. Whereas most previously reported V2V measurement campaigns were performed using "regular" antenna arrays put in an elevated position on the car (e.g., on the roof), our antenna antenna arrays were specifically designed for V2V communications, which includes integration into the existent radome ("shark fin") on the car roof (see [9] for further details). The radome cavity, which is shared with antennas for other applications such as GSM and FM radio, can be regarded as a likely position for a real application. The antenna arrays were designed such that their elements were linear in the longest dimension of the radome. Since this implies that the array would being parallel to the direction of travel, we rotated the radome 90 degrees such that the array orientation and the driving direction were perpendicular. The subsequent analysis makes use of the middle elements of the array, elements 2 and 3, whose antenna patterns have their main gain in the forward and backward direction (see Fig. 1).

The measurement locations are documented by means of GPS coordinates recorded by the Tx and Rx cars. Additionally, videos were recorded for each measurement, to enable identification of important scatterers and provide refined information on the exact whereabouts of the cars during the measurements.

B. Measurement Environment

In order to draw conclusions about the importance of different propagation mechanisms, we performed measurements in four different types of intersections (see Fig. 2). The main difference lies in the availability of a LOS component and the location and density of significant scatterers (such as other buildings and vehicles). The following intersections, with GPS coordinates given, were measured:

(a) **Open** (N55°41.710′, E13°11.323′) – A four-way intersection in Lund, without buildings in direct proximity to it. In this scenario, the LOS component should thus be (more or less) constantly available. There are traffic lights and the intersecting streets are two-lane, with additional turn lanes. Traffic is busy during measurements and the scattering environment is rich with e.g., street signs, flag poles, parked cars and a metal fence next to the road. For practical reasons (mainly due to the intervals of traffic lights), timing was very complicated in this scenario resulting in a measurement time window covering rather the leaving than the approaching of the intersection.

(b) **Single building** (N55°42.448′, E13°9.658′) – A two-way intersection in Lund, with a four-story building in the quadrant next to the intersecting streets. The distance from the building to the road center is 9–14 m. The streets are single-lane without traffic lights and there was no traffic (except the rare occurrence of a bus) during the measurements. The remainder of the area bordering the intersection is more or less empty, containing a few distant one-story parking garages, some vegetation and a power transmission line. This scenario is thus expected to experience difficult channel conditions in the absence of LOS.

(c) **Narrow urban** (N55°42.627′, E13°11.257′) – A four-way intersection in Lund, Sweden, with four-story buildings in each quadrant and no traffic lights. The distance from the buildings to the road center is 14–17 m and there is a single lane in each direction. There is some traffic during the measurements and there are also parked cars along the road side in all directions. This scenario is expected to provide many possible propagation paths in the absence of LOS between Tx and Rx.

(d) **Wide urban** (N55°35.947′, E13°0.518′) – A four-way intersection in Malmö, Sweden, with two-lane traffic in each direction, traffic lights and four-story buildings in all quadrants. There are also additional turn lanes in all directions (for both right- and left-turns), and there was busy traffic during the measurements. The distance from the building to the road center is 20–43 m. Similar to the previous scenario, this intersection is expected to provide many possible propagation paths, and the wider streets are expected to imply an earlier occurring LOS path. The traffic situation makes this scenario the most dynamic.

During each measurement, the transmitter (Tx) and receiver (Rx) cars approached the crossing from perpendicular directions at a speed of $30 - 40$ km/h, in scenarios (b)–(d) with a building blocking the (optical) LOS path. Several measurements were made in each scenario, with the cars approaching from different combinations of the intersecting streets.

III. Data Evaluation

To analyze the channel properties, we derive the time-varying average power delay profile (APDP) for each Tx/Rx link (array element combination) as

$$P_\tau(\tau, t) = \frac{1}{N_t} \sum_{n=0}^{N_t-1} \left| h(\tau, t + n\Delta t) \right|^2, \qquad (1)$$

where $h(\tau, t)$ is the time-varying channel impulse derived by an inverse Fourier transform of $H(f, t)$ (a Hann window was

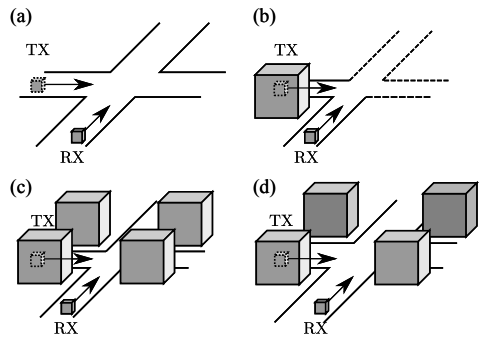

Fig. 2. Principle structure of the four intersections. Intersections (a) and (d) are wider than (b) and (c).

used to suppress sidelobes) and $N_t \Delta T$ was set to 57 ms, corresponding to a Tx (or Rx) movement of 10 wavelengths at 35 km/h. From the APDPs, we derive the time-varying, small-scale averaged channel gain as

$$G(t) = \sum_{\tau} P_\tau(\tau, t). \quad (2)$$

In this process, we apply a noise threshold by setting all components of $P_\tau(\tau, t)$ that are weaker than 2 dB above the noise floor to zero. We thus let the channel gain include antenna gain/losses, which is reasonable since we are using a realistic antenna configuration. The channel gain can therefore be directly used to determine the expected output from the receiver antenna. We also determine the time-varying rms delay spread as the second central moment of the APDP [10].

In order to analyze the signal contribution from individual scatterers, we use the two-step tracking algorithm described in [11]. First, a high resolution search-and-subtract method is applied in order to refine the delay estimates of the different paths, then paths are tracked over time and delay such that the time-varying power of a path can be analyzed.

IV. Results

In this section, we analyze the measurement results and draw conclusions about the most important propagation mechanisms. We pay special attention to the differences between the four types of intersections.

APDPs for the four different types of intersections are shown in Figs. 3 to 6. Our first observation is that each APDP consists of several identifiable "lines," i.e., contributions that are present over several consecutive time instants (typically on the order of seconds). This structure has been observed in several previous V2V measurement campaigns, e.g., [4], [11]. These *discrete* multipath components (MPCs) usually stem from the reflection off a single scattering object, e.g., a vehicle or a building, which can offer a possible propagation path over a long time duration. In addition to the discrete MPCs, the APDPs also contain a *diffuse* contribution, i.e., MPCs that do not show a temporal coherence.

The open intersection (a) has the richest channel of the four intersections; several discrete as well as diffuse contributions can be seen in Fig. 3. This is not surprising, since the constant availability of LOS in this scenario leads to a multitude

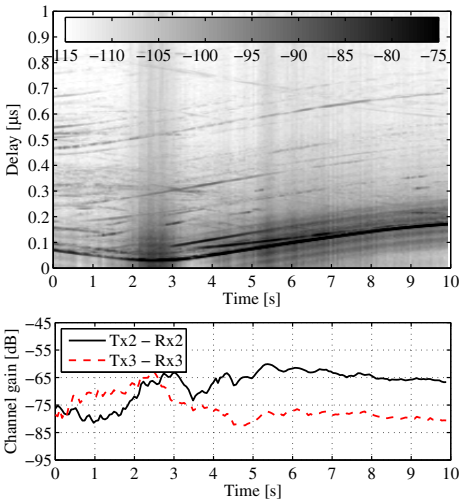

Fig. 3. Average power delay profile for Tx2-Rx2 (top) and channel gain for Tx2-Rx2 and Tx3-Rx3 (bottom) for the open intersection (a).

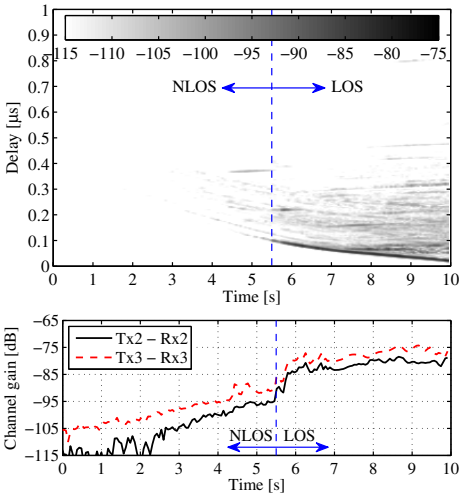

Fig. 4. Average power delay profile for Tx2-Rx2 (top) and channel gain for Tx2-Rx2 and Tx3-Rx3 (bottom) for the single building intersection (b).

of other propagation paths. The channel gain is high in this scenario, indicating that a V2V message for a collision avoidance system is likely to go through.

The APDP from the intersection with a single building (b) in Fig. 4 is in stark contrast to that of intersection (a). We find that the channel is very poor before LOS is obtained, which is reasonable since there are very few objects that can offer additional propagation paths in this scenario. This could be problematic for a collision avoidance system, especially when small-scale fading is also considered.

Fig. 5 shows an APDP for the narrow urban intersection (c). We find that similar to intersection (b), the signal level is poor for early time instants (i.e., far away from the intersection), though generally slightly higher than for the single-building intersection. In this intersection, however, the channel gain shows a steeper increase as the intersection is approached, and a few discrete components start to become visible in the APDP even before LOS is obtained. The number of visible discrete MPCs is still interestingly low at this point, especially

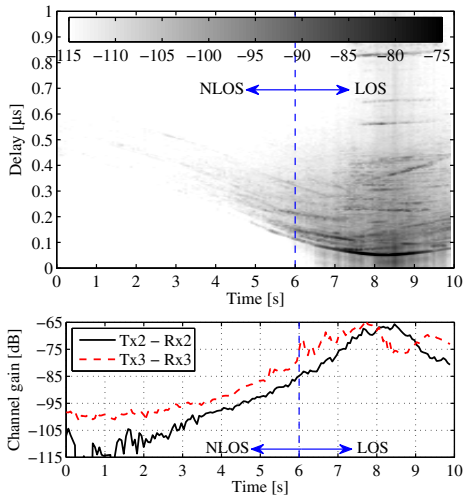

Fig. 5. Average power delay profile for Tx2-Rx2 (top) and channel gain for Tx2-Rx2 and Tx3-Rx3 (bottom) for the narrow urban intersection (c).

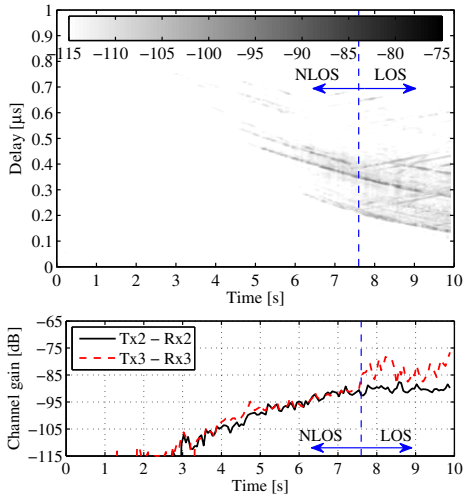

Fig. 6. Average power delay profile for Tx2-Rx2 (top) and channel gain for Tx2-Rx2 and Tx3-Rx3 (bottom) for the wide urban intersection (d).

given the number of available scattering objects (there are e.g., parked cars along all streets). It is also noteworthy that between 7.5 s and 9.5 s, when both cars are in the intersection, a whole range of other discrete MPCs become visible, many of them at relatively large delays. These MPCs stem from far away scattering objects further down the intersecting roads. At this point, the APDP resembles that of intersection (a).

An APDP from the wide urban intersection (d) is shown in Fig. 6. This APDP is very sparse, essentially consisting of only a few discrete MPCs. Considering the physical environment, we conclude that also here, very few of the large number of possible scattering objects (e.g., the multitude of cars that are waiting at the traffic lights in every direction) actually contribute to the received signal when approaching the intersection. The ones that do, however, render MPCs that are visible for a relatively long duration before LOS is obtained. We analyze the two longest paths in detail: the ones visible from 5 s to 9 s and 5 s to LOS, respectively.

To determine the origin of these discrete MPCs, we make

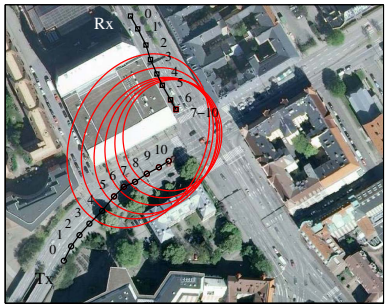

Fig. 7. Scattering ellipses for the first arriving discrete MPC before LOS is obtained in Fig. 6. The markers indicate the positions of the Tx and Rx with a one second interval; the Rx is waiting at a red light during last three seconds of the measurement. The ellipses are shown for the six last seconds of the measurements, which is the time window during which the MPC is visible.

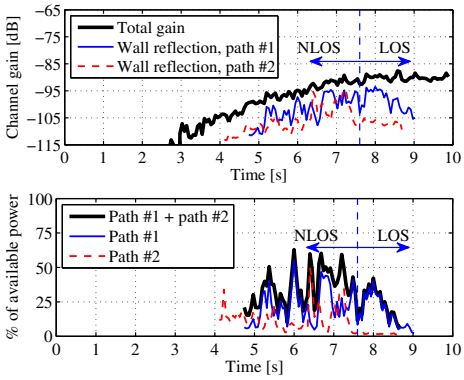

Fig. 8. Tracked power for the two discrete MPCs before LOS in Fig. 6 (top) and the amount of the total power accounted for by these paths (bottom).

use of the documentation data (videos and GPS coordinates) to acquire knowledge of the Tx and Rx location at each time instant, and thus the theoretical LOS path. Knowing the propagation delay between the LOS path and the MPC from the APDP, we can draw, for each time instant when the MPC is visible, the scattering ellipse corresponding to this additional delay on a map of the intersection. The procedure is demonstrated in Fig. 7 for the first arriving of the two paths. If the source of the path is a single bounce off a point scatterer in the horizontal plane, the scatterer must be located on the intersecting point of the ellipses. Even though these assumptions are not necessarily fulfilled for all occasions, the procedure works remarkably well in the majority of the cases we analyze, in the sense that realistic results are the outcome. From Fig. 7, we conclude that the first of the two analyzed MPCs is a reflection in the horizontal plane from the building left of the Rx car. Similarly, we find that the second path likely is a single-bounce off the roof edge of the same building.

Using the tracking algorithm, we extract the time-varying power of these MPCs. The result is shown in the upper plot of Fig. 8 and we conclude that a lot of the received power is due to these reflections. The lower plot of Fig. 8 shows that in the absence of LOS, up to $50 - 60\%$ of the total power is due to the building left of the Rx.

In order to simplify comparison between the different intersections, as well as put the channel gain into context of

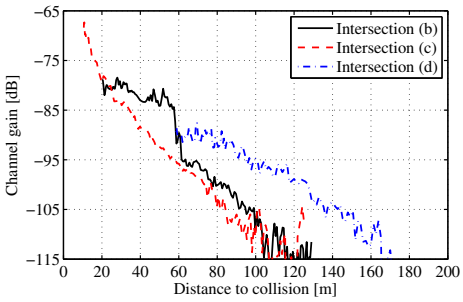

Fig. 9. Channel gain as a function of the combined distance to collision for the Tx2 to Rx2 link.

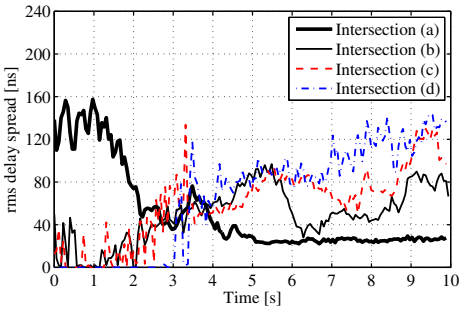

Fig. 10. Calculated rms delay spread for the Tx2 to Rx2 link for all four intersections.

collision avoidance applications, we want to somehow relate the different intersections. We do this by defining the *combined distance to collision*, d_{dc}, as the aggregated distance from Tx and Rx, respectively, to the point in the intersection where they would collide. The distance to collision thus relates to the commonly used *forewarn time*, t_{f}, by $t_{\mathrm{f}} = d_{\mathrm{dc}}/(2v_{\mathrm{av}})$, where v_{av} is the average speed of the Tx and Rx. In the comparison, we exclude intersection (a) since the amount of recorded data during the approaching of the intersection is too small (using the time window when the cars are leaving the intersection would constitute an unfair comparison since the forward and backward antenna gains are not equal). The result is plotted in Fig. 9, where it can be seen that the intersection that provides the strongest signal actually is the wide urban intersection (d). Intersections (b) and (c), on the other hand, somewhat surprisingly show very similar curves, at least up until LOS occurs. The effect of LOS is obviously interwoven in the result: in intersection (c), LOS occurs only when the cars are very close to each other, whereas LOS is available from a larger distance in intersections (b) and (d). Interestingly enough, the difference in channel gain between (b)/(c) and (d) is $3-4$ dB before LOS is obtained, which roughly corresponds to the amount of signal power made available by the building left of the Rx in intersection (d).

The evaluated rms delay spreads for the different intersections are shown in Fig. 10 and we find that the delay spread shows considerable variations over time. For intersections (b) and (c), the delay spread has a local minimum just after the LOS path becomes available. As the cars approach the intersection further, the delay spread increases again due to more propagation paths becoming available. The latter effect is especially pronounced for intersection (c), where the delay spread reaches its maximum when both cars are in the intersection, as a consequence of far away scatterers becoming available at this point (as discussed previously). The same observation holds for intersection (a). The delay spread of intersection (d) is, somewhat counterintuitively, constantly increasing as the cars approach the intersection, due to an increasing number of available propagation paths.

V. Summary and Conclusions

This paper presented results from a vehicle-to-vehicle measurement campaign for collision avoidance applications and our findings demonstrates the challenges that such systems may encounter. We found that the channel pathloss is strong when the vehicles are far away form the intersection, with few physical objects actually providing propagation paths. Comparing the results from different intersections, we noted that in the absence of line-of-sight, the coverage is dependent on the availability of significant scatterers such as buildings, which may account for a large fraction of the received power. We also discovered that the number of available propagation paths increases dramatically when both cars are in the intersection, leading to the rms delay spread being maximal at this instant.

References

[1] J. Kunisch and J. Pamp, "Wideband car-to-car radio channel measurements and model at 5.9 GHz," in *Proc. IEEE Veh. Technol. Conf. 2008 fall*, Sep. 2008.

[2] L. Cheng, B. Henty, D. Stancil, F. Bai, and P. Mudalige, "Mobile vehicle-to-vehicle narrow-band channel measurement and characterization of the 5.9 GHz dedicated short range communication (DSRC) frequency band," *IEEE J. Sel. Areas Commun.*, vol. 25, no. 8, pp. 1501–1516, Oct. 2007.

[3] I. Sen and D. W. Matolak, "Vehicle-vehicle channel models for the 5-GHz band," *IEEE Trans. Intell. Transp. Syst.*, vol. 9, no. 2, pp. 235–245, Jun. 2008.

[4] O. Renaudin, V.-M. Kolmonen, P. Vainikainen, and C. Oestges, "Wideband MIMO car-to-car radio channel measurements at 5.3 GHz," in *Proc. IEEE Veh. Technol. Conf. 2008 fall*, 2008.

[5] A. Paier, J. Karedal, N. Czink, C. Dumard, T. Zemen, F. Tufvesson, A. Molisch, and C. Mecklenbräuker, "Characterization of vehicle-to-vehicle radio channels from measurements at 5.2 GHz," *Wireless Personal Commun.*, vol. 50, pp. 19–29, 2009.

[6] G. Acosta-Marum and M. Ingram, "Six time- and frequency- selective empirical channel models for vehicular wireless lans," *IEEE Veh. Technol. Mag.*, vol. 2, no. 4, pp. 4–11, Dec. 2007.

[7] Z. He, W. Chen, W. Zhou, M. Pätzold, and A. Chelli, "Modelling of MIMO vehicle-to-vehicle fading channels in T-junction scattering environments," in *Proc. European Conf. Antennas Prop.*, 2009, pp. 652–656.

[8] I. Tan, W. Tang, K. Laberteaux, and A. Bahai, "Measurement and analysis of wireless channel impairments in DSRC vehicular communications," in *Proc. IEEE Int. Conf. Commun.*, 2008, pp. 4882–4888.

[9] A. Thiel, O. Klemp, A. Paier, L. Bernadó, J. Karedal, and A. Kwoczek, "In-situ vehicular antenna integration and design aspects for vehicle-to-vehicle communications," in *Proc. European Conf. Antennas Prop.*, 2010.

[10] A. F. Molisch, *Wireless Communications*. Chichester, West Sussex, UK: IEEE Press–Wiley, 2005.

[11] J. Karedal, F. Tufvesson, N. Czink, A. Paier, C. Dumard, T. Zemen, C. F. Mecklenbräuker, and A. F. Molisch, "A geometry-based stochastic MIMO model for vehicle-to-vehicle communications," *IEEE Trans. Wireless Commun.*, vol. 8, no. 7, pp. 3646–3657, Jul. 2009.